Comparison between FLO-2D and Debris-2D on application of assessment of granular debris flow

AUTHOR(S):

Liu, Ko-Fei; Wu, Ying-Hsin

Comparison between FLO-2D and Debris-2D on application of assessment of granular debris flow

Ko-Fei Liu (*Dept. of Civil engineering, National Taiwan University, Taiwan*)
Ying-Hsin Wu (*Dept. of Civil engineering, National Taiwan University, Taiwan*)

Abstract In Taiwan, numerical simulation has been a widely accepted method for assessment of debris flow hazard. The most used numerical programs are FLO-2D and Debris-2D. Even though these two programs are applied to the same engineering tasks, but they are different in many aspects. We compare these two programs according to their fundamental theories, input and output data, computational algorithms and results. A real debris flow with abundant granular material induced by landslides at Xinfa village in southern Taiwan is simulated by both programs for comparison. As shown by simulation results, Debris-2D gives better result in hazard area delineating and flow depth predicting than FLO-2D. Therefore, granular debris flows are better simulated by Debris-2D.
Keywords. debris flow assessment, program comparison, FLO-2D, Debris-2D

1. Introduction

In debris flow hazard assessment, numerical simulation is widely used for delineation of the affected area. FLO-2D and Debris-2D (Liu and Huang, 2006) programs are the most used one in Taiwan. FLO-2D is a commercially available software for two-dimensional flood or mud-flood routing, and is published by FLO-2D Software Inc. since 1993. FLO-2D is capable of simulating flow depth, flow velocity and affected area of flood and mud flow on plains, creeks, alluvial fans, channels, or other artificial surfaces. It has been listed on the Federal Emergency Management Agency (FEMA, USA) list as the approved hydraulic programs for flood and debris flow simulation.

In 1993, FLO-2D was first applied to simulate the mudflow event of the Rudd creek in Utah, USA on urbanized area (O'Brien et al. 1993). However, the simulation doesn't give reasonable affected area compared with field measurements. As the only commercially available tool, FLO-2D has been widely applied for the assessment of debris flow hazard since then. To use FLO-2D, one has to calibrate several hydraulic parameters as well as the discharge hydrograph. Usually, this calibration procedure could produce accepted results on the spread but not the flow depth for debris flows. Chen et al. (2004) simulated the affected zone of the debris flow induced by breaching of a landslide dam; Lin et al. (2005) assessed the debris flow hazard of the Chuishe creek in the Chen-you-lan watershed, Nantou, Taiwan. Bertolo and Wieczorek (2005) analyzed the debris flows in the Yosemite National Park, California, USA. Četina et al. (2006) conducted the numerical simulation of debris flow induced by landslides in the Stože Mountain in northwest Slovenia. Hsu et al. (2010) assessed and delineated the debris-flow hazard zone in Hualien, Taiwan. But even with calibrated inputs, the simulated results may not match with the field as in Boniello et al. (2010) or Stolz and Huggel (2008). With the affected area obtained, many has applied it to the evacuation planning and vulnerability and risk assessment (Chen et al., 2004; Lin et al., 2008; Chen et al., 2009; Lin et al., 2011; Quan Luna et al. 2011). But there is no record for FLO-2D to made any successful predictions of a hazard before it occurs.

Different from FLO-2D that can be applied for flood routing, Debris-2D is only used for two-dimensional debris flow simulation and delineation. Debris-2D program was developed and first appeared in 2006. Liu and Huang (2006) used this program to simulate the debris flow hazard in Nantou County, Taiwan. Compared with the field measurements, the simulated results had less than 5% error in affected area as well as the final height

of deposition. Then, Liu and Wu (2010) assessed the debris flow event in Inje, northeast South Korea in 2006, and the simulation result of flow depth and distribution agrees with the field investigation very well. There are several successful prediction by Debris-2D. For example, Debris-2D was applied to assess the debris flow affected area in Daniao tribe southeast Taiwan in 2006 and the simulation agrees very well with the real event occurred in 2009 (Tsai et al., 2011). No calibration is needed to use Debris-2D, all parameters must be decided according to guidelines. Debris-2D is also applied for vulnerability risk assessment (Liu and Lee, 2007; Tsai et al., 2010) and mitigation design evaluation (Liu et al., 2009).

In this study, we first introduce the governing equations, input, computational algorithm and input data for FLO-2D and Debris-2D separately. Then, a real case is simulated for comparison.

2. Introduction of FLO-2D

The text written in this section comes from the user manual of FLO-2D (2006), but only the portion related to debris flow is mentioned.

2.1 Governing equations

In two-dimensional plane, there are eight flowing directions defined in FLO-2D program. They are east, west, south, north, southeast, southwest, northeast and northwest directions. In each direction, the constant density fluid is assumed to be hydrostatic. The governing equations are continuity and dynamic wave momentum equation, in each direction. For example, the x direction government equations are

$$\frac{\partial H}{\partial t}+\frac{\partial\left(uH\right)}{\partial x}=i\,, \tag{1}$$

$$\underbrace{S_f}_{\substack{\text{friction}\\ \text{slope}}} = \underbrace{S_0}_{\substack{\text{gravity}\\ \text{slope}}} - \underbrace{\frac{\partial H}{\partial x}}_{\substack{\text{pressure}\\ \text{term}}} - \underbrace{\frac{u}{g}\frac{\partial u}{\partial x}}_{\substack{\text{convective}\\ \text{term}}} - \underbrace{\frac{1}{g}\frac{\partial u}{\partial t}}_{\substack{\text{acceleration}\\ \text{term}}}\,, \tag{2}$$

where x and t are spatial and temporal independent variables respectively. Dependent variables H and u are flowing depth and depth-averaged velocity in x-direction. g is the gravitational acceleration. S_f and S_0 are bottom friction and bed slope respectively. i is excess rainfall intensity. If there is no rainfall, i.e. i = 0, Eqs. (1) and (2) are reduced to the famous Saint-Venant equations.

Friction slope S_f is calculated using stresses. In modeling mud or debris flow, there are five components in shear stress

$$\tau=\tau_c+\tau_{mc}+\tau_v+\tau_t+\tau_d\,, \tag{3}$$

where τ_c is cohesive yield stress; τ_{mc} is Mohr-Coulomb shear; τ_v is viscous shear stress; τ_t and τ_d are turbulent and dispersive shear stress respectively. The constitutive law for shear stress and strain-rate used is

$$\tau=\tau_y+\eta\left(\frac{\partial u}{\partial y}\right)+C\left(\frac{\partial u}{\partial y}\right)^2\,, \tag{4}$$

where $\tau_y=\tau_c+\tau_{mc}$ and η is dynamic viscosity [unit: poise]; the turbulent-dispersive coefficient C is

$$C=\rho_m l^2+\frac{\pi}{12}\left(\frac{6}{\pi}\right)^{1/3}\sin^2\left(\alpha_I\right)\rho_s\left(1-e_n{}^2\right)C_v{}^{1/3}\,. \tag{5}$$

Equation (4) is similar to the model proposed by Julien and Lan (1991), but Julien and Lan model gives zero strain rate for stress less than yield stress while Eq. (4) does not. ρ_s is density of debris. ρ_m is density of mixture. e_n is energy restitution coefficient. α_I is averaged impact angle of solid. From Eq. (4), the friction

slope S_f can be obtained as

$$S_f = \underbrace{\frac{\tau_y}{\gamma_m H}}_{S_y} + \underbrace{\frac{K\eta u}{8\gamma_m H^2}}_{S_v} + \underbrace{\frac{n_{td}{}^2 u^2}{H^{4/3}}}_{S_{td}}, \tag{5}$$

where S_y and S_v are yield stress and viscous slope respectively, and $S_y + S_v$ represents the effects of yield stress and viscosity; S_{td} is turbulent-dispersive slope and stands for the collision effects between solids; K is resistance parameter. τ_y is yield stress and n_{td} is turbulent flow resistance. They can be expressed as

$$\tau_y = \alpha_2 \exp\left(\beta_2 C_v\right), \tag{6}$$

$$\eta = \alpha_1 \exp\left(\beta_1 C_v\right), \tag{7}$$

$$n_{td} = n_t b \exp\left(m C_v\right), \tag{8}$$

where b = 0.0538 and m = 6.0896; n_t is turbulent n-value. The values of K, η and n_t can be found in the user manual (FLO-2D, 2006).

2.2 Program inputs

For simulating debris flow, the main inputs are topography and friction coefficients. FLO-2D uses DEM with square uniform grids. In each gird, constant Manning's n value is used to represent the property of surface friction. No bottom erosion or deposition is considered. Man made structure can be input into FLO-2D, the effect can be included in the simulation.

The inputs for debris-flow are rainfall hydrograph, debris-flow discharge hydrographs with corresponding inflow locations and rheological parameters. The rainfall hydrograph is obtained through rainfall record during the debris-flow event. The debris-flow discharge hydrograph includes water runoff hydrograph and the temporal variation of solid volume concentration C_v (%). The volume concentration C_v ranges from 0.45 to 0.55 according to user manual (FLO-2D 2006). The fixed inflow location corresponding to each debris-flow inflow needs to be prescribed. Every grid element can be assigned to be the inflow location. The needed rheological parameter inputs include specific weight γ_m, yield stress τ_y, dynamic viscosity η and turbulent flow resistance n_{td}. In the limit of water, user can input C_v = 0. Then from Eq. (6), $\tau_y = \alpha_2$. The value of α_2 can be found from user manual of FLO-2D, and the value is between 0.1 and 0.01.

2.3 Computational algorithm of FLO-2D

The space derivatives in FLO-2D governing equations are discretized by central difference method. The Newton-Raphson method is applied in time to solve the depth-averaged velocity u_i^{t+1} and the discharge Q_i^{t+1} in each flowing direction, where the superscript $t+1$ and subscript i represent the next time step and eight different flowing directions respectively. Summing discharges in eight directions, total volume net change can be obtained for next time by

$$\Delta Q_i^{t+1} = \sum_{i=1}^{8} Q_i^{t+1} . \tag{9}$$

Then, the net change of flow depth at next time step is

$$\Delta d_i^{t+1} = \frac{\Delta Q_i^{t+1} \Delta t}{A_{surf}}, \tag{10}$$

where Δt and A_{surf} are time step and surface area of the grid element respectively. With Eq. (10) and values of flow depth from previous time step, flow depth at next time step, $t+1$, can be obtained. The averaging in Eq. (9) can also be used to smooth shock wave or hydraulic jump during the computation (FLO-2D, 2006).

According to the variation of inflow hydrograph, the time step Δt will be changed. For a steep rising hydrograph, the time step will decrease for the stability of computation; otherwise, time step can increase to speed up the computation (FLO-2D, 2006). The termination mechanism for simulation is the maximum simulation time input by user. There is no physical mechanism or other conditions in program to terminate the simulation.

2.4 Outputs

The default output time interval is hour. Output in minutes can be done with the finest resolution. The output data include temporal variation of flow depth, flow velocity and impact force. Maximum flow depth and velocity are also recorded. FLO-2D has a very convenient and friendly user interface. All the output can be converted into ESRI shapefile automatically for displaying in geographic information system (GIS).

3. Introduction to Debris-2D

3.1 Governing equations

The governing equations are mass and momentum conservation with shallow water assumption. The coordinate system is the Cartesian coordinate with the average bed elevation as x axis. The adopted constitutive relation is the 3-D generalization form proposed by Julien and Lan (1991), as below:

$$\tau_{ij} = \left(\frac{\tau_0}{\varepsilon_{II}} + \mu_d + \mu_c \varepsilon_{II} \right) \varepsilon_{ij} , \qquad \text{for} \quad \tau_{II} \geq \tau_0 , \tag{11}$$

$$\varepsilon_{II} = 0 , \qquad \text{for} \quad \tau_{II} < \tau_0 , \tag{12}$$

where $i, j = x, y, z$ and

$$\varepsilon_{II} = \left(\frac{1}{2} \varepsilon_{ij} \varepsilon_{ij} \right)^{1/2} , \quad \tau_{II} = \left(\frac{1}{2} \tau_{ij} \tau_{ij} \right)^{1/2} \quad \text{and} \quad \varepsilon_{ij} = \frac{1}{2} \left(\frac{\partial u_i}{\partial x_j} + \frac{\partial u_j}{\partial x_i} \right) .$$

ε_{ij} is strain-rate tensor; τ_0 is yield stress; μ_d and μ_c are dynamic viscosity and turbulent-dispersive coefficient respectively. Eq. (11) represents the constitutive relation in the shear layer where the shear stress is greater than yield stress; Eq. (12) is for the plug layer that the shear stress is less than yield stress.

From the analysis of field data, Liu and Huang (2006) find that the shear layer thickness is less than 10% of total flow depth. So the shear layer can be ignored to the leading order. After simplification, the resulting governing equations in conservative form are conservation of mass

$$\frac{\partial H}{\partial t} + \frac{\partial (uH)}{\partial x} + \frac{\partial (vH)}{\partial y} = 0 , \tag{13}$$

and conservation of momentum in *x*- and *y*-directions

$$\frac{\partial (uH)}{\partial t} + \frac{\partial (u^2 H)}{\partial x} + \frac{\partial (uvH)}{\partial y} = -gH \cos\theta \frac{\partial B}{\partial x} - gH \cos\theta \frac{\partial H}{\partial x} + gH \sin\theta - \frac{1}{\rho} \frac{\tau_0 u}{\sqrt{u^2 + v^2}} , \tag{14}$$

$$\frac{\partial (vH)}{\partial t} + \frac{\partial (uvH)}{\partial x} + \frac{\partial (v^2 H)}{\partial y} = -gH \cos\theta \frac{\partial B}{\partial y} - gH \cos\theta \frac{\partial H}{\partial y} - \frac{1}{\rho} \frac{\tau_0 v}{\sqrt{u^2 + v^2}} , \tag{15}$$

where $H = H(x, y, t)$ is flow depth; $B = B(x, y)$ is bed topography which assumed to be fixed; *u* and *v* are depth-averaged velocities in *x*- and *y*-direction respectively, and they are functions of spatial variables *x*, *y* and temporal variable *t*; θ is the averaged bottom bed slope; τ_0 and ρ are debris-flow yield stress and density, which are all assumed to be constant; *g* is the gravitational acceleration. The version of Debris-2D compared here is the early version. This version does not consider bottom erosion and deposition. Since the bottom shear

layer is ignored, the yield stress becomes the dominant bottom stress in this version.

Now we can compare Eq. (4) and Eq. (11) and (12). Debris-2D treats constitutive relation as a nonlinear discontinuous relation while FLO-2D treats it only as part of the bottom stress and a continuous concept. With nonlinear treatment, Debris-2D can derive the initiation criterion for any originally stationary debris pile. This is the initiation condition

$$\left(\frac{\partial B}{\partial x}+\frac{\partial H}{\partial x}-\tan\theta\right)^2+\left(\frac{\partial B}{\partial y}+\frac{\partial H}{\partial y}\right)^2>\left(\frac{\tau_0}{\rho g\cos\theta H}\right)^2. \tag{16}$$

The derivative of B and H represent pressure effect and $\tan\theta$ is the gravitational effect. The right hand side is the resistance from yield stress. As is shown in Eq. (16), debris flow can move only if pressure and gravitational effects exceed the yield stress effects.

3.2 Input data

The main inputs are topography and initial debris source distribution. Different from FLO-2D, the grid for Debris-2D can be rectangular grids. There is no need for Manning's n value, but an accurate value for yield stress must be measured from samples. But for a rough estimation, yield stress value can be estimated with grain size and composition. Man-made structures can be included and modified into the DEM for simulation.

The debris distribution must be found through field survey, aerial or satellite photos. From the field survey or satellite photo analysis, one can find the dry debris volume V_d and its corresponding locations. From Takahashi (1991) the solid volume concentration C_v (%) of a flowing debris flow can be expressed as

$$C_v=\frac{\rho\tan\theta}{(\sigma-\rho)(\tan\phi-\tan\theta)}, \tag{17}$$

where ρ is water density; σ is the density of dry debris (around 2.65 g/cm^3); ϕ is internal friction angle (about 37◦) ; θ is average bottom slope angle in the field. The maximum value of C_v cannot exceed 0.603. With C_v obtained from Eq. (18), the volume of the flow V_d can be calculated as V_d / C_v. These source volumes and their locations can be input to the original DEM through the user interface.

The only rheological parameter needed for input is the yield stress τ_0. Its value varies according to the solid size and composition in the field, and usually ranges from 102 Pa to 104 Pa for debris flows with large granular materials. The larger the averaged grain diameter, the higher the yield stress. For mud flows, the yield stress is usually less than 100.

3.3 Computational algorithm

Finite difference method is applied to discretize the governing equations, i.e. Eqs. (14), (15) and (16). In space, the 1st-order Upwind method is applied to discretize convective term and 2nd-order central difference method is used for the remaining terms. The explicit 3rd-order Adams-Bashforth method is used for time advancing.

To start the computation, Debris-2D will determine where debris flow can be initialized by Eq. (16). If Eq. (16) is not satisfied, the mass stays stationary and velocities are zero with the flow depth unchanged. Time step Δt is fixed in Debris-2D. During computation, if the maximum velocity in the whole computation domain is less than numerical error, the computation terminates.

3.4 Output data

The output time interval of Debris-2D can be in seconds. Similar to FLO-2D, Debis-2D can output temporal variation of flow depth, depth-averaged velocities in the whole domain. Debris-2D can also calculate impact force (Liu and Lee 1997; Liu et al. 1997) for specified locations, the final affected area and the maximum flow depth and velocities in time.

Table 1 Comparison between FLO-2D and Debris-2D

Attribute		FLO-2D	Debris-2D
Category	Item		
Fundamental Theory	Governing equation	Mass and momentum equations in 8 directions	Mass and momentum equations in conservative form
	Constitutive relation	Julien and Lan (1991)	
	Initiation criterion	No	Derived
	Shock treatment	Direction average	Damping scheme
Input Data	DEM	Uniform and square grids in x, y directions	Grids in x, y directions
	Manning's n value	Needed	Not necessary
	Rainfall hydrograph	From rainfall data	Not necessary
	Debris flow mass	Discharge hydrograph (calibrated)	Mass distribution from field survey
	Debris flow Inflow location	Predefined as initial input	Not necessary
	Initial mass distribution	Not necessary	Needed from field or from aerial photo
	Landslide location effect	Through hydrograph and debris flow inflow location	Mass distribution input according to landslide location
	Input parameters	Volume concentration C_v, yield stress τ_y, viscosity η, Manning's n value, Resistance parameter K, turbulent flow resistance n_{td}, etc.	Yield stress τ_0
Computational Algorithm	Numerical scheme in space	Central difference method	1st-order Upwind method for convective term,)
	Numerical scheme in Time (Δt)	Forward difference (Time step adjusted through CFL)	3rd-order Adam-Bashforth method for time differencing (Time step fixed)
	Stopping mechanism	User defined maximum simulation time	Flow stops automatically during calculation (yield stress τ_0 effect)
	Volume conservation	Conserved	
Output	Output data	Temporal variation of Flow depth, depth-averaged velocities in whole domain, maximum flow depth and impact force of time variation	
	Time resolution	hour	second
Program interface and functionality		Complete and friendly	Complete but not yet friendly

4. Comparisons between FLO-2D and Debris-2D

An overall comparison between FLO-2D and Debris-2D is listed in Tab.1. Physically, Derbis-2D can simulate the starting and termination of debris flows. Flows in FLO-2D cannot stop unless user terminates the computation artificially.

Numerically, Debris-2D treats shocks better than FLO-2D due to the use of upwind method and conservative form of equations. But in computation efficiency, FLO-2D uses variable time steps but Debris-2D uses fixed time step. Therefore, FLO-2D is more efficient in CPU time.

The most significant difference is the input of debris flow volume. FLO-2D uses the user defined debris flow discharge hydrographs and treats debris flow (or mud flow) as flood routing. Debris-2D simulates the flowing motion with real source distributions determined through field survey or satellite photo analysis. As a result, a landslide induced debris-flow event should be better simulated by Debris-2D. The method for termination of simulation can have dramatically effect on the affected zone. Since FLO-2D is terminated through user defined maximum time of calculation, the final spread of debris flow can be different for different simulation time. But Debris-2D terminates simulation by physical criteria, the final spreading of debris flow will not be affected by simulation time.

The outputs from both programs are similar, with minor difference on output time interval. But FLO-2D has a friendly interface and well developed link to graphical user interfaces (GUI) and geophysical information system (GIS). Even Debris-2D has the GUI program for use, the interface still needs improvement.

5. Case study

5.1 Introduction of the field case

In order to validate and compare the two programs, a real case occurred during typhoon Morakot in Xinfa village, southern Taiwan (Fig. 1) is studied. Typhoon Morakot hit Taiwan on August 5-10, 2009 and brought world record heavy rainfall. There were severe floods, countless landslides, and debris flow disasters associated with Typhoon Morakot. The catastrophic landslide in Xiaolin village (Tsou et al. 2011) is one among many disasters. There are 673 deaths, 26 people missing, and about 70 million US dollars of agricultural and property loss induced by Typhoon Morakot and is the worst typhoon disaster in 20 years in Taiwan.

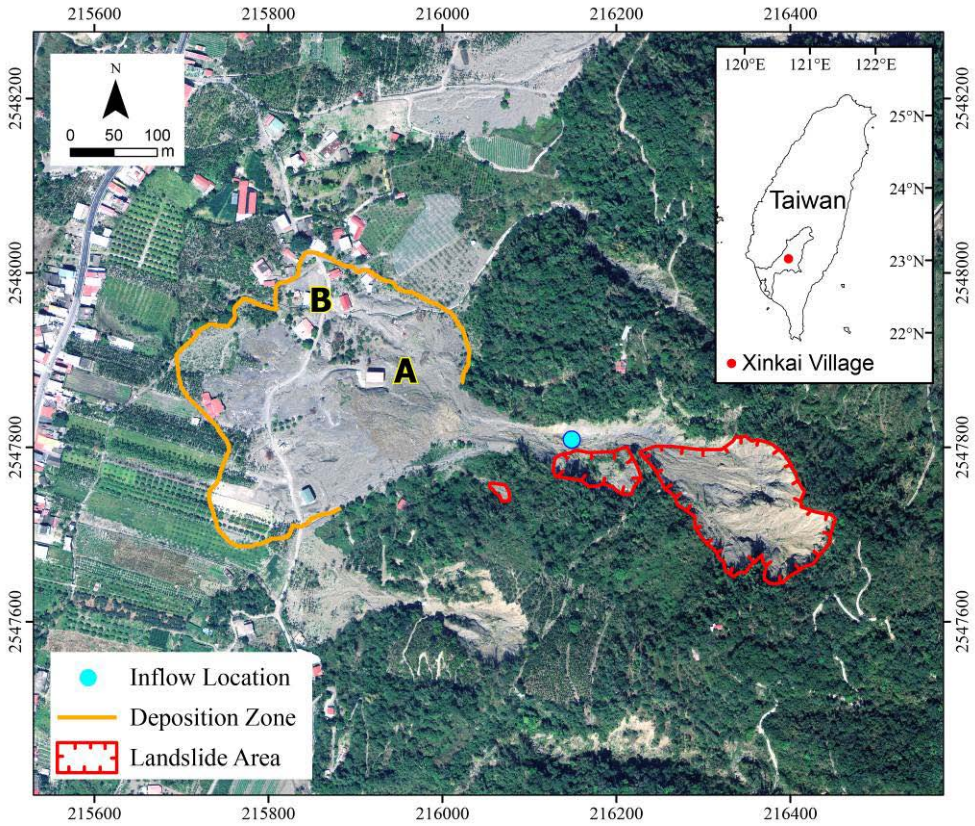

Fig. 1 Aerial photo of Xinfa Village (shooting time: 2010/3). The region circled by red line is landslide area, and orange for deposition zone. The location marked ● is the inflow location for FLO-2D simulation. The marks A and B are buried houses, also see the zoom-in photo in Fig. 8.

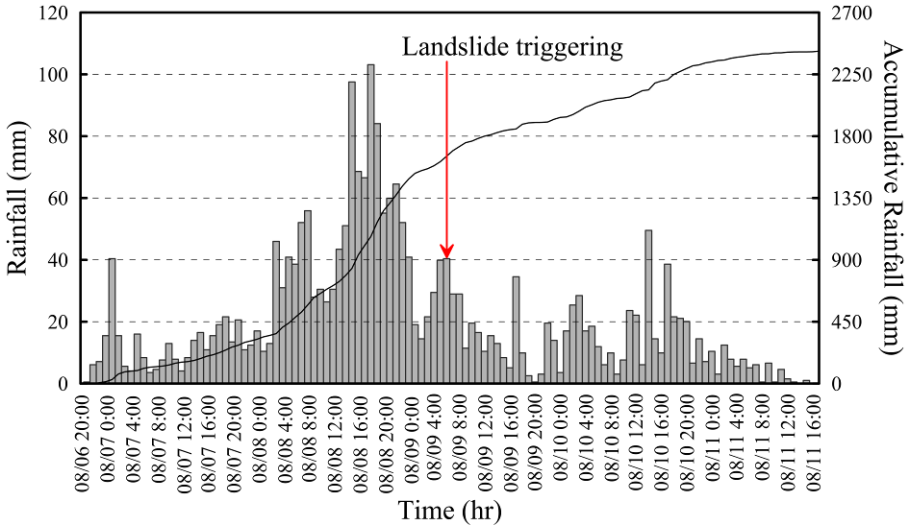

Fig. 2 The hourly and accumulative rainfall hydrograph recorded by Xinfa meteorological station (No. C1V240, Central Weather Bureau of Taiwan), the unit is mm. The triggering time of the landslide was at 6 AM on August 9, 2009.

Table 2 Input data of FLO-2D and Debris-2D for Xinfa village case study (†FLO-2D User manual, 2006)

Attribute		FLO-2D	Debris-2D
Category	Item		
Topography	DEM resolution	5m × 5m	
	Manning's n value†	$n = 0.03$ for riverbed $n = 0.1$ for farm land $n = 0.04$ for road & artificial surfaces	Not necessary
Parameters input	Volume concentration	$C_v = 0.603$ (%)	
	Yield stress	$\alpha_2 = 0.0723$, $\beta_2 = 20$ for Eq. (6)	$\tau_0 = 1,250$ (Pa)
	Viscosity	$\alpha_1 = 0.05$, $\beta_1 = 20$ for Eq. (7)	Not necessary
	Resistance parameter K	2,000	Not necessary
	Specific weight	2,650 (kg/m^3)	
	Simulation time	10 hours	2 hours
Debris flow input	Initial mass distribution	Not necessary	Fig. 4 (a)
	Water discharge hydrograph	see Scenario I and II in Fig. 3	Not necessary

Xinfa village landslide and debris flow is one of the disasters. The rainfall hydrograph is shown in Fig. 2 and was recorded at the Xinfa meteorological station. This station is 2.2 km away from the disaster location. The accumulative rainfall in 5 days exceeds the average local annual accumulative rainfall 2,398 mm. At 6:00 AM on August 9, landslides in eastern part of Xinfa village occurred and induced debris flows. There were 5 people dead, 12 people injured, 6 houses buried, and about 15 Hectare destroyed agriculture area. The orthorectified aerial photo, which was taken six months after the disaster, of landslide and the final deposition area are shown in Fig. 1. The three landslide areas are, from right to left, 21,183; 3,562 and 285 m^2 respectively, as is circled by red lines in Fig. 1. According to the field survey (SWCB, 2010), the total volume of debris deposition is about 130,000 m^3. From field examination, debris flow traces can be clearly identified in local buildings, one of the trace is shown in Fig. 5. The height of the trace indicated that debris flow passed that particular building at a height about 6 m and the location of this house is marked A in Fig. 1.

The major lithological formation in Xinfa village is the Chaochoiu formation with weakly deformed rocks of

argillite and slate which are clipped by quartzite sheets. In the field, the weathered rocks form onion-skin-like weathering shape or pencil structure (Lin et al., 2011), and fractures usually occur along the foliation. The grain size of the weathering rocks are relatively small, i.e. ≤ 50 mm, and the rocks compose of clay or silty clay and gravels with the structure of leaf or pencil. As the frictional forces among these debris are relatively large, this material possesses higher yield stress. So the value of 1,250 Pa for yield stress is used in all simulations.

5.2 Input data

For complete listing of inputs for both programs, please see Tab. 2. There are common inputs. The topography input is DEM in resolution of 5m×5m. For both simulations the value of yield stress is 1,250 Pa, and the solid volume concentration C_v is 0.603 from Eq. (17). With C_v and the total debris 130,000 m^3, we obtain the total volume of debris flow is about 215,600 m^3. In what follows we describe the input for FLO-2D and Debris-2D separately.

FLO-2D considers infiltration. But the debris flow occurred on the third day of the typhoon event, the accumulation rainfall is already 2,754 mm, so we assume that all the debris and soil are saturated at that time. So the infiltration effect is negligible. The discharge hydrograph and inflow locations are needed for FLO-2D. The inflow location is at the downstream of landslide and is marked as ● in Fig. 1. Referring to literatures (Stolz and Huggel, 2008; Lin et al, 2008), we assume two triangular form discharges hydrographs of different duration as the inflow inputs for FLO-2D simulation. The two hydrographs of Scenario I and II are shown in Fig. 3. The duration of Scenario I is 1 hour, and 2 hour for Scenario II. The peak of the hydrograph is determined by the total debris flow volume as 215,600 m^3, so the peak values of Scenario I and II are 33.75 and 16.88 cms respectively. The total simulation time for both scenarios is 10 hour.

As for mass input in Debris-2D, we distribute the debris-flow mass, of which the total volume is 215,600 m^3, on the three landslide areas by constant but different depth. The initial mass distribution is shown in Fig. 4a.

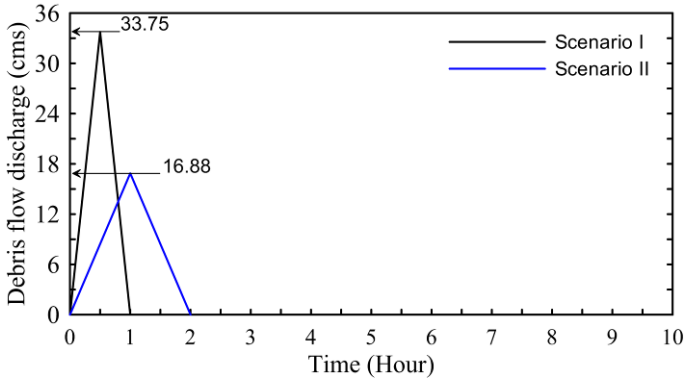

Fig. 3 Hydrographs of debris flow discharge for Scenario I and II at the inflow location marked by blue circle ● in Fig. 1. The duration of discharge is 1 hour. For Scenario I and II, the peak values of discharge are 33.75 and 16.88 cms respectively. For both scenarios for FLO-2D simulation, the total simulation time is 10 hours.

5.3 Simulation results and discussion

The simulation results of FLO-2D for Scenario I and II are displayed at 1, 2, 3 and 10 hour as shown in Fig. 5. From the simulation results, only the simulated result from Scenario II at 2 hr agrees reasonablely with the in-situ deposition , see Fig. 5f. However, at this time, the maximum velocity of debris flow remains 0.07 m/s, and the distribution still grows as time goes by, see Fig. 5g and h. From the results of two scenarios, we find that the simulated distribution grows wider and wider in time. This result also proves that FLO-2D will not terminate the simulation automatically. One has to know what the best termination time of simulation is in order to get a reasonable result. But the question of which hydrograph and which termination time should be used are unknown unless there is a disaster occurred already. So FLO-2D cannot be used for prediction at all.
The simulated flow depth of both scenarios at the buried house location marked as A in Fig. 1 are shown in Fig.

6. The maximum flow depth of Scenario I and II are only 3.49 and 2.86 m respectively. Both simulated depths are much less than the real in-situ depth 6.5m as see Fig. 8.

The results of Debris-2D are shown in Fig. 8, and the whole debris flow event is finished in 163 seconds which agrees with the real disaster. The depth distributions at time 0 (initial), 10, 20, 30, 60, 163 second are shown in Fig. 4 respectively. The final deposition area coincides well with the affected area (black boundary). From the aerial photo, the maximum error is 39.4 m and the error is less than 13% with respect to the final transverse spread. The temporal flow depth variation at the buried house (marked A in Fig. 1) is shown in Fig. 7. The maximum depth is about 6.53 m at 16.3 second, and this depth agrees well with the in-situ measurement in Fig. 8. The simulated final deposition depth at the front (line B in Fig. 5) is about 2~3 m, and agrees with field condition well. The duration of the whole event is close to 3 minutes and also fits the local residents' description. As the simulation results show, Debris-2D gives better simulation results.

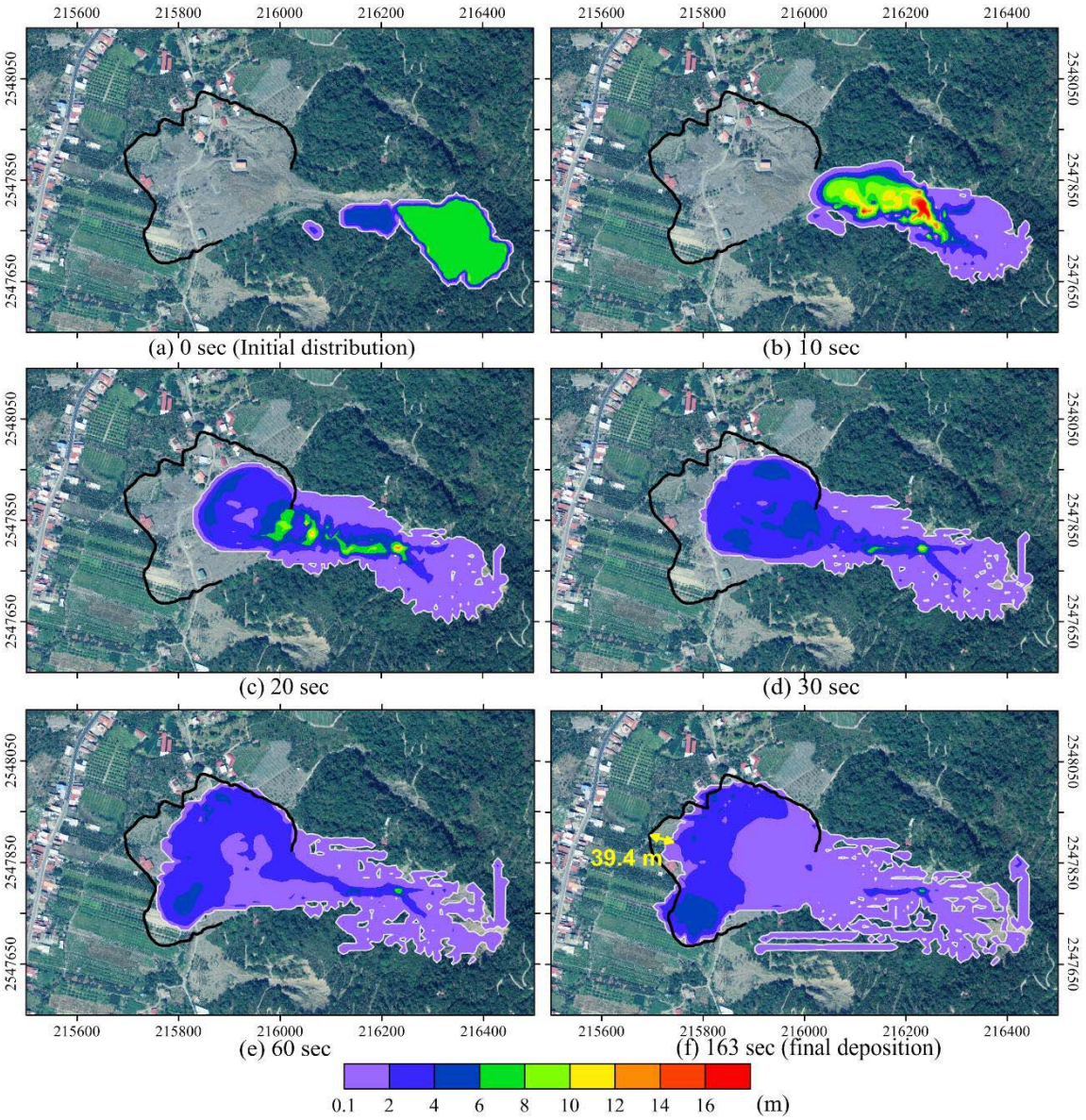

Fig. 4 The simulation results using Debris-2D at different time. The black line represents the front of the deposition zone. In (f), the maximum difference between the simulated and in-situ front location is 39.4 m.

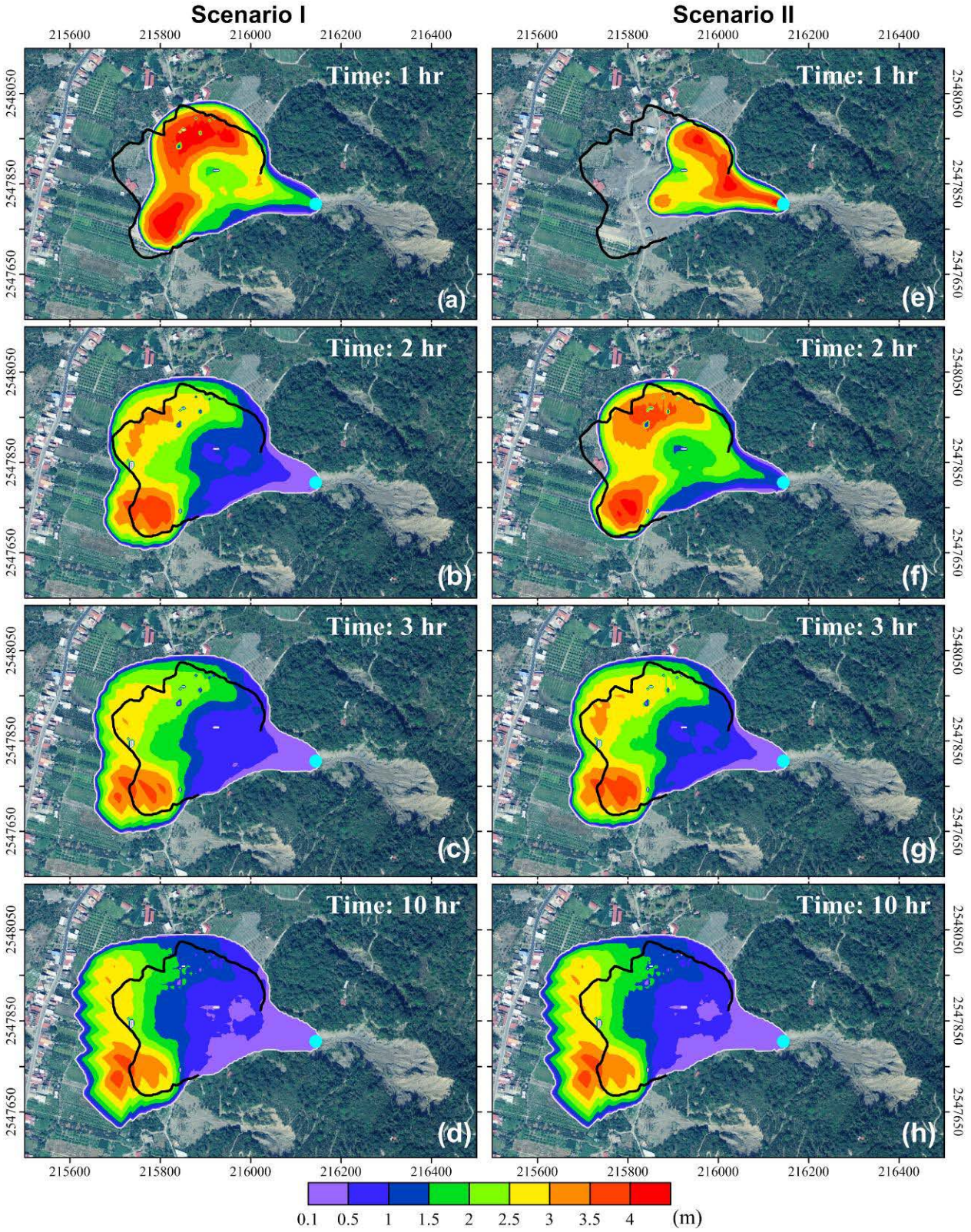

Fig. 5 The simulation results of Scenario I and II using FLO-2D at different time. The black line represents the front of the deposition zone. The mark • is the inflow location.

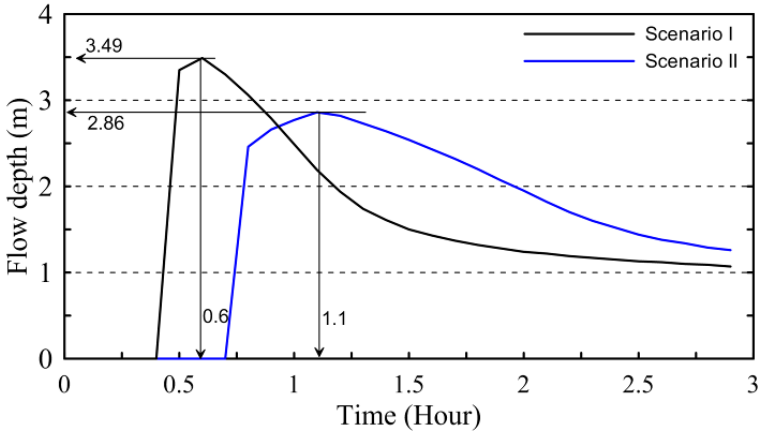

Fig. 6 The flow depths of time variation obtained by FLO-2D simulation at the location of the buried house, as is marked A in Fig. 1. In Scenario I, at 0.6 hour the maximum depth is 3.49 m; In Scenario II, the maximum depth is 2.86 at 1.1 hour. Both simulated depths are far from the real in-situ depth 6.5m, as in Fig. 8.

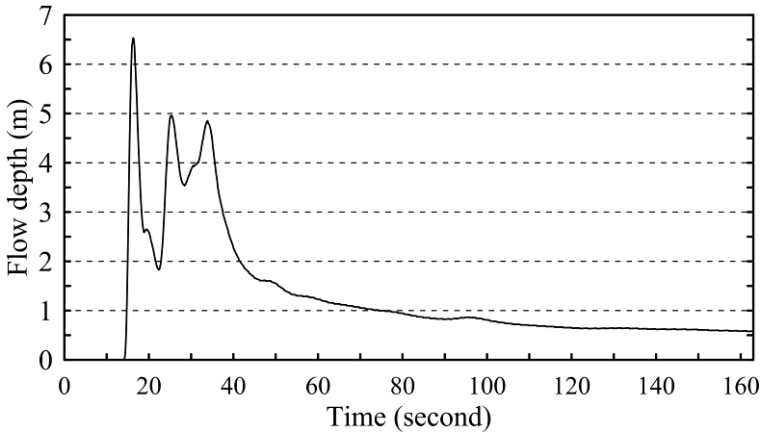

Fig. 7 The temporal variation of flow depth obtained by Debris-2D simulation at the location of the buried house, as is marked A in Fig. 1. At 16.3 second, the maximum depth is 6.53 m, and it matches the in-situ condition, see Fig. 8.

Fig. 8 Photo of the buried houses where the photo was taken toward northwest from the location marked A in Fig. 1. At the location A, from the trace on the wall, the flow depth of debris flow is about 6m at least. The deposition depth of the debris flow front is about 2~3 m, as shown at the location B.

6. Concluding remarks

This paper compares FLO-2D and Debris-2D for the applicability of debris flows with a lot of granular material. The theories used are different, but the major difference is the different methods in treating rheological relations. As a result, very different simulation termination mechanisms are used by two programs. FLO-2D is a flow routing program, so a termination condition is usually not required. For usage in debris flows, one has to artificially terminate the simulation. But debris flows do stop, so simulation from Debirs-2D does display this characteristic.

From the results of a real case study, the mass distribution simulated by FLO-2D does not agree with the field nor depth distribution. But the final distribution and maximum depth simulated from Debris-2D agree with the field very well. Since the case in this paper has a lot of granular material, so the comparison can only stand for debris flows with a lot of granular material. Therefore, application on assessment of debris-flow hazards, Debris-2D is recommended for landslide-triggered debris-flow hazard. However, the input from debris-2D can be obtained even before a disaster occurs. But FLO-2D needs the real disaster information in order to perform any simulation. This feature means Debris-2D can be used for prediction and FLO-2D can not.

Acknowledgments

The financial support provided by National Science Council of Taiwan (under grant No. NSC 96-2625-Z-002 -006-MY3) is appreciated.

References

Boniello, M.A., Calligaris, C., Lapasin, R. & Zini, L., 2010. Rheological investigation and simulation of a debris-flow event in the Fella watershed. Natural Hazards and Earth System Sciences 10.5, 989–997.

Bertolo, P., Wieczorek, G.F., 2005. Calibration of numerical programs for small debris flows in Yosemite Valley, California, USA. Natural Hazards and Earth System Science 5.6, 993–1001.

Chen, C.Y., Chen, T.C., Yu, F.C., Hung, F.Y., 2004. A landslide dam breach induced debris flow-a case study on downstream hazard areas delineation. Environmental Geology 47, 91–101.

Chen, S.C., Wu, C.Y., Wu, T.Y., 2009. Resilient capacity assessment for geological failure areas: examples from communities affected by debris flow disaster. Environmental Geology 56, 1523–1532.

Chen, S.C., Wu, C.Y., Huang, B.T., 2007. Risk assessment of debris flow disaster in Songhe village. Journal of Chinese Soil and Water Conservation 38.3, 287–298. (in Chinese)

Četina, M., Rajar, R., Hojnik, T., Zakrajšek, M., Krzyk, M., Mikoš, M., 2006. Case study: numerical simulations of debris flow below stoze, Slovenia. Journal of Hydraulic Engineering ASCE 132.2, 121–129.

FLO-2D Software, Inc., 2006. FLO-2D Users manual (version 2006.01), Arizona, USA.

Hsu, S.M., Chiou, L.B., Lin, G.F., Wen, H.Y., Kuo, C.Y., 2010. Applications of simulation technique on debris-flow hazard zone delineation: a case study in Hualien County, Taiwan. Natural Hazards and Earth System Science 10, 535–545.

Hydrologic Engineering Center, US Army Corps of Engineers, 2010. Hydrologic Modeling System, HEC-HMS Version 3.5 User's Manual.

Julien, P.Y., Lan, Y., 1991. Rheology of hyperconcentrations. Journal of Hydraulic Engineering ASCE 117.3, 346–353.

Lin, D.G., Hsu, S.Y., Chao, C.H., Wen, H.Y., Hsu, S.M., Ku, C.Y., Chi, S.Y., 2008. Applications of simulation technique on hazard zone delineation and damage assessment of debris flow. Journal of Chinese Soil and Water Conservation 39.4, 311–319. (in Chinese)

Lin, C.W., Lin, W.H., Kao, M.C., 2011. Geological map of Taiwan scale 1:50,000. Central Geological Survey, Ministry of Economic Affairs, R.O.C. (in chinese)

Lin, M.L., Wang, K.L., Huang, J.J., 2005. Debris flow run off simulation and verification - case study of Chen-You-Lan watershed, Taiwan. Natural Hazards and Earth System Science 5, 439–445.

Lin, J.Y., Yang, M.D., Lin, B.R., Lin, P.S., 2011. Risk assessment of debris flows in Songhe Stream, Taiwan. Environmental Geology 123, 100–112.

Liu, K.F., Lee, F.C., 1997. Experimental analysis on impact mechanism of granular flow. Chinese Journal of Mechanics 13.1, 87–100. (in chinese)
Liu, K.F., Lee, F.C., Tsai, S.P., 1997. The flow field and impact force on a debris dam. Proceedings of the First International conference on Debris-flow Hazards Mitigation: Mechanics, Prediction, and Assessment, 737–746.
Liu, K.F., Li, H.C., Hsu, Y.C., 2009. Debris flow hazard defense magnitude assessment with numerical simulation. Natural hazards 49.1, 137–161.
Liu, K.F., Li, H.C., 2007. The assessment of debris flow emergency measures. Journal of City and Planning 34.1, 57–73. (in chinese)
Liu, K.F., Wu, Y.H., 2010. The Assessment of Debris Flow Hazard in Korea Using Debris-2D. INTERPRAEVENT 2010-International Symposium in Pacific Rim, Taiwan.
Liu, K.F., Huang, M.C., 2006. Numerical simulation of debris flow with application on hazard area mapping. Computational Geoscience 10, 221–240.
O'Brien, J.S., Julien, P.Y., Fullerton, W.T., 1993. Two-dimensional water flood and mudflood simulation. Journal of Hydraulic Engineering ASCE 119.2, 244–260.
Quan Luna, Q., Blahut, J., van Westen, C.J., Sterlacchini, S., van Asch, T.W.J., Akbas, S.O., 2011. The application of numerical debris flow programling for the generation of physical vulnerability curves. Natural Hazards and Earth System Science 11, 2047–2060.
Soil and Water Conservation Bureau, 2010. The Investigation of vulnerability factors and risk analysis of debris flow potential creeks, Soil and Water Conservation Bureau, Taiwan. (in chinese)
Stolz, A., Huggel, C., 2008. Debris flows in the Swiss National Park: the influence of different flow programs and varying DEM grid size on programing results. Landslides 5, 311–319.
Tsai, M.P., Hsu, Y.C., Li, H.C., Shu, H.M., Liu, K.F., 2011. Applications of simulation technique on debris flow hazard zone delineation: a case study in Daniao tribe, Eastern Taiwan. Natural Hazards and Earth System Science 11, 3053–3062.
Takahashi, T., 1981. Debris flow. Annual Review of Fluid Mechanics 13, 57–77.
Tsou, C.Y., Feng, Z.Y., Chigira, M., 2011. Catastrophic landslide induced by Typhoon Morakot, Shiaolin, Taiwan. Geomorphology 127, 166–178.

K.F. Liu
Dept. of Civil, Collage of Engineering.
National Taiwan University, Taiwan
No.1, Sec. 4, Roosevelt Rd., Taipei 10617, Taiwan
e-mail: kfliu@ntu.edu.tw

Y.H. Wu
Dept. of Civil, Collage of Engineering.
National Taiwan University, Taiwan
No.1, Sec. 4, Roosevelt Rd., Taipei 10617, Taiwan
e-mail: d95521016@ntu.edu.tw